

Numerical Modeling of the Tissue Freeze-Thaw Cycle during Cutaneous Cryosurgery using Liquid Nitrogen Spray

Feng Sun¹, G. -X. Wang^{1*}, K. M. Kelly², G. Aguilar³

¹Department of Mechanical Engineering, The University of Akron, Ohio 44325

²Beckman Laser Institute, University of California, Irvine, CA 92612-1475

³Department of Mechanical Engineering, University of California Riverside, CA 92521

ABSTRACT

It is common in some cryosurgical procedures to rely on freeze-thaw cycle(s) to destroy undesirable tissues. Most research in cryosurgery focuses on the freezing process and much less attention has been paid to thawing or re-warming. However, as ice melts during thawing, the extracellular solution can become locally hypotonic, driving water into cells, resulting in cell expansion and ultimately, membrane rupture. Therefore, the thermal history of the target tissue during both the freezing and thawing processes is critical for cell viability. To better understand and predict the thermal history during cryosurgery, we developed a two-dimensional numerical model to describe the complete freeze-thaw cycle during liquid nitrogen cutaneous cryosurgery. A stratified anatomical structure of human skin is considered in the model. The numerical simulation applies temperature-dependent thermal and physical properties for human skin tissue and considers the typical thermal boundary conditions for clinical practice. Parametric studies are performed to explore the influence of spray cooling, spray duration and surface heating. Results are discussed concentrating on iceball front propagation, lethal temperature isotherm evolution, tissue temperature variation and cooling rates. These results are expected to provide both quantitative and graphical support to cutaneous cryosurgery and suggest approaches to optimize current cryosurgical protocols.

Keywords: Cutaneous cryosurgery, bioheat transfer, tissue freezing.

INTRODUCTION

Cryosurgery using freezing to destroy undesired tissues is extensively used by dermatologists for removal of diverse benign and malignant cutaneous lesions [1]. Compared to alternative treatment modalities, cutaneous cryosurgery has many merits including: (i) a brief treatment period; (ii) bloodless treatment field; (iii) a good cosmetic result with minimal scarring; (iv) ease of performance; (v) high cure rate and (vi) low cost [2]. With these profound advantages, cutaneous cryosurgery has witnessed widespread acceptance in dermatological clinical practice for treatment of a wide range of skin lesions including actinic keratosis, warts, hypertrophic scars, keloids, mucoceles and solar lentigos [3].

Several techniques have been developed for cutaneous cryosurgery, including swab, probe and spray methods. The swab method uses a cotton-tipped applicator saturated with LN₂ and applies LN₂ directly onto the target skin surface. Histological and thermal studies have demonstrated that freezing induced by swab technique cannot destroy cells located deeper than 1.5 mm from skin surface. This is inadequate for treatment of thick tumors [4]. Cryoprobe, a closed system with continuous circulation of LN₂, was first developed by Dr. Irving Cooper in 1961 and has been widely applied in cryosurgeries of several anatomic areas including the liver and prostate. Spray method utilizes a canister to store LN₂ and changeable nozzles to spray LN₂ onto the skin surface. For the majority of cutaneous cryosurgery, the spray technique is preferred because of ease of use and the potential for

* Corresponding author: gwang@uakron.edu

relatively deep tissue destruction as compared to the swab method [5].

A successful cryosurgical process requires careful monitoring and evaluation of the freezing front. Otherwise, insufficient or excessive freezing may occur resulting in incomplete lesion destruction and malignancy recurrence or unnecessary destruction of healthy tissue. Many researchers have been working to develop mathematical models to predict the extent and thermal history of tissue freezing during cryosurgery [6-9]. However, most research concentrated on the tissue freezing process induced by single or multiple cryoprobes, and few of them described the LN₂ spray method. Further, single or multiple freeze-thaw cycles have been routinely used in cryosurgery. However, the thawing process has rarely been evaluated despite its important contribution to cellular damage due to bio-physical interactions, like recrystallization of intracellular ice and water transportation through cell membranes [10].

Applying two-dimensional finite volume formulation, the present study uses apparent heat capacity method to simulate thermal history and phase change processes in human skin for a single freeze-thaw cycle. Instead of bulk tissue, the stratified structure of human skin is implemented in the model. The results can be used for clinical pretreatment planning and for design of optimal cryosurgery protocols.

NOMENCLATURE

C	heat capacity, J/Kg·K;
h	convective heat transfer coefficient, W/m ² ·K;
k	thermal conductivity, W/m·K;
L	latent heat, J/Kg;
p	penetration depth, mm;
\dot{q}	heat generation rate, W/m ³ ;
R_0	spray cooling site radius, mm;
r	radial coordinate, mm;
T	temperature, °C;
t	time, sec.;
z	axial coordinate, mm;

Greek

α	thermal diffusivity, m ² /s;
ρ	mass density, Kg/m ³ ;
ξ, η	switch variables valuing 0 or 1;
τ	dimensionless time;
$\dot{\omega}$	blood perfusion rate, sec. ⁻¹ ;

Subscript

a	air;
b	blood;
epi	epidermis;
f	frozen
m	metabolic;
$m1$	liquidus;
$m2$	solidus;
s	spray;
u	unfrozen

MATHEMATICAL MODEL SETUP

Human skin consists of a stratified structure of three distinct parallel strata: epidermis, dermis and subcutaneous fatty tissue. Epidermis is the most superficial stratum of the skin. The most superficial layer of the epidermis is the stratum corneum, which is made up of dead keratinized cells. Underneath are several layers of keratinocyte cells, which comprise the bulk of the epidermis. The dermis is a dense connective tissue layer with a rich blood and nerve supply. Subcutaneous fatty tissue is dominated by fat cells and perfused by parallel arteriole/venule pairs.

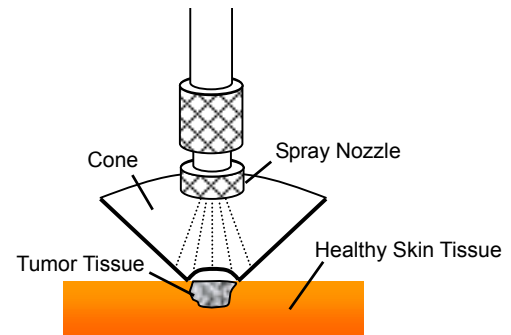


Figure 1. Schematic of cutaneous cryosurgery using LN₂ spray.

For LN₂ cutaneous cryosurgery spray method, the nozzle is positioned 1 to 1.5 cm from the skin surface and is aimed at the center of the target lesion, as schematically shown in Figure 1 [6]. A cone shield may be used to confine the spray to the desired area and prevent undesired exposure of surrounding healthy skin. When the spray gun is triggered, a combination of nitrogen gas and fine droplets of LN₂ impinge onto the skin surface and an LN₂ film forms. Due to strong vaporization of the LN₂, the target skin tissue is rapidly cooled. When the temperature of the skin drops down to the tissue phase change temperature, the freezing process starts. An iceball develops through the epidermis into the dermis and eventually encompasses the tumor. Once the spray is stopped, if there is no external heat source, the frozen tissue will be warmed up by surrounding unfrozen tissue and slow thawing will occur. Spray induced freezing and subsequent thawing are routinely described as the freeze-thaw cycle, which leads to cellular destruction and tissue injury by the following mechanisms [11]: dehydration and resulting concentration of electrolytes; crystallization and consequent rupture of cellular membranes; denaturation of the lipid-protein molecules within the cell membrane; thermal shock and vascular stasis.

It is generally accepted that two physical processes, heat transfer and phase change, dominate the tissue freeze-thaw cycle during cryosurgery. Delineated by phase change fronts, heat transfer domain in the tissue can generally be divided into three regions as schematically illustrated in Fig. 2, where regions I, II and III represent the unfrozen region, phase change region (i.e. mushy region) and frozen region, respectively. The unfrozen region is distinguished by two biophysical processes in living tissue: metabolism and blood perfusion. It is therefore

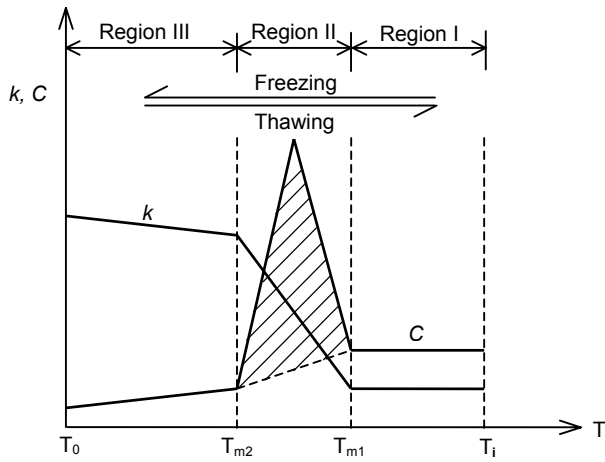


Figure 2. Schematic presentation of the temperature-dependent thermal properties applied in the study.

customary to describe the heat transfer within the unfrozen region by the classical Pennes bioheat equation [7]. The phase change region (mushy zone) exists because biological tissues are non-ideal materials and the phase change process occurs over a relatively wide temperature range. Being highly tissue type dependent, the upper limit of the range (T_{m1}) may vary between $-0.5\text{ }^{\circ}\text{C}$ and $-1\text{ }^{\circ}\text{C}$, and the lower limit (T_{m2}) between $-5\text{ }^{\circ}\text{C}$ and $-10\text{ }^{\circ}\text{C}$ [8]. During the freezing process, phase change latent heat is liberated within this region. Blood perfusion is believed to cease when the tissue is cooled down to T_{m1} , and metabolism stops when tissue temperature drops to T_{m2} . During the thawing process, the frozen tissue absorbs latent heat and the iceball melts. Blood perfusion resumes when the tissue is warmed up to T_{m1} and the partial recovery of metabolism happens at T_{m2} depending on the viability of the tissue.

Cutaneous cryosurgery is a complicated physical process involving complex bio-physical interactions as well as heat transfer mechanisms, including multiphase LN_2 spray convection and evaporation, heat exchange between the skin surface and LN_2 , and latent heat release/absorption during phase change. The present study quantifies the effects of spray cooling and convective warming on skin tissue and determines a thermal history of targeted cells. The process is simplified by employing a series of assumptions:

- (1) The LN_2 spray cone is assumed to be circular with uniform spray cooling within the impingement area. This allows simulation of heat transfer and phase change in the skin using an axisymmetric geometry system, as shown in Fig. 3. It is noted that, in reality, the heat transfer within the spray cone may vary in the radial direction [12].
- (2) Skin tissue is treated as a three-layer structure with homogeneous properties for each layer. The skin tissue takes 37°C as the initial uniform temperature. The specific heat, the thermal conductivity, and the latent heat are estimated from the mass fraction of water within the tissue [13].

- (3) Phase change and metabolism are neglected for the epidermis, and metabolic heat generation is assumed to be zero for subcutaneous fat during the cryosurgery.
- (4) Metabolism is assumed to recover completely for the dermis when the tissue warms up to T_{m2} , since exploratory calculation finds that the treatment does not produce significant difference to tissue thermal history during thawing process.
- (5) Microscopic biophysical processes such as cell dehydration, intracellular ice formation (IIF) and vascular injury are not considered.
- (6) Lesional and non-lesional tissues are assumed to share identical thermal properties.
- (7) The apparent specific heat of the solid/liquid mixture within the phase change range is assumed to vary linearly.

Based on the above assumptions, a mathematical equation for modeling heat transfer in each of the three layers can be written as:

$$\rho_i C_i \frac{\partial T}{\partial t} = \nabla(k_i \cdot \nabla T) + \xi \dot{\omega}_b \rho_b C_b (T_b - T) + \eta \dot{q}_m \quad (1)$$

where the subscript i denotes the epidermis, dermis and subcutaneous fat, respectively; b stands for blood and m metabolism. ρ_b and C_b are set to 1060 Kg/m^3 and $3.84\text{ KJ/Kg}\cdot\text{K}$, respectively, for blood mass density and heat capacity [14]. Coefficients ξ and η function as switch variables to control blood perfusion and metabolic heat generation effects for the three layers during the freeze-thaw cycle. The values of ξ and η are assigned according to anatomic structure and function of human skin and listed in Table 1. $\dot{\omega}_b$ and \dot{q}_m are calculated referring to Table 2.

Table 1. Assignment of ξ and η for three layers during freeze-thaw process.

Region	Epidermis	Dermis	Fat
Unfrozen	$\xi = 0; \eta = 0;$	$\xi = 1; \eta = 1;$	$\xi = 1; \eta = 0;$
Mushy	$\xi = 0; \eta = 0;$	$\xi = 0; \eta = 1;$	$\xi = 0; \eta = 0;$
Frozen	$\xi = 0; \eta = 0;$	$\xi = 0; \eta = 0;$	$\xi = 0; \eta = 0;$

Table 2. Thermal physical properties of the three layers used in computation (from [14] if not otherwise indicated).

Properties	Epidermis	Dermis	Fat
k_u (W/m·K)	0.2	0.498	0.268
k_f (W/m·K)	0.2	$(273-T)^{1.156}$ $\times 0.0039 + 1.463$ ^(a)	0.268
C_u (J/Kg·K)	3530	2721	2400
C_f (J/Kg·K)	3530	$89.7 + 5.04T$	2400
ρ (Kg/m ³)	1500	1116	916
L (J/Kg)	0	217100	70808
\dot{q}_m (W/m ³)	0	1240 ^(b)	0
$\dot{\omega}_b$ (1/s)	0	0.002387 ^(b)	0.002387 ^(b)

^(a) calculated from [17]; ^(b) calculated from [19].

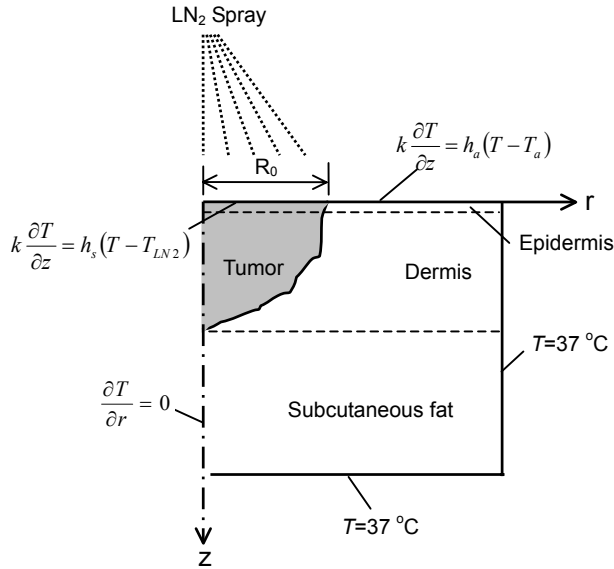


Figure 3. Illustration of computation domain and boundary conditions during freezing.

The computational domain and boundary conditions are schematically illustrated in Fig. 3, where the shaded area represents the skin tumor. The domain consists of three layers: epidermis (0.1 mm thick), dermis (3 mm) and subcutaneous fat. It is assumed that the spray cone radius impacting on the skin surface, $R_0 = 5$ mm, is the same as the pathologic radius of the tumor at the skin surface. The spray duration, t_s , considered in computation is 30s, since it is commonly used in clinical practice [6]. When the spray starts, LN_2 induced cooling is represented by a convective heat transfer coefficient, h_s ; while outside of the spray cone, heat is supplied to the skin surface from room air with a much smaller convective heat transfer coefficient, h_a . h_a is also used to represent the convective warming by ambient air during the thawing process:

$$k_{epi} \left. \frac{\partial T}{\partial z} \right|_{z=0} = \begin{cases} h_s [T(r,0,t) - T_{LN2}] & 0 \leq r \leq R_0; 0 < t \leq t_s \\ h_a [T(r,0,t) - T_a] & R_0 < r; 0 < t \leq t_s \\ h_a [T(r,0,t) - T_a] & r \geq 0; t > t_s \end{cases} \quad (2)$$

where k_{epi} is the epidermis thermal conductivity, T_{LN2} is the temperature of LN_2 at the skin surface, taken as -196°C (the saturated temperature of LN_2 at atmospheric pressure), and T_a is room air temperature, 27°C . Assuming the temperature of muscle or structures underneath the subcutaneous fat are not affected during cryosurgery, all other boundaries are set at human body temperature (e.g., $T = 37^\circ\text{C}$).

The commercial CFD software package, FLUENT (Fluent, New Hampshire), is used to solve the above mathematical problems. An apparent heat capacity method is used to treat the phase change process. The numerical method is first validated by solving a 1-D water-ice phase change process in half-space. The water at an initial uniform temperature, $T_i = 20^\circ\text{C}$, is confined to a semi-infinite space $x > 0$. At time $t = 0$, the boundary surface at $x = 0$ is lowered to a temperature, $T_0 = -50^\circ\text{C}$, and maintained. As such, solidification starts at the surface $x = 0$ and the ice front moves in the positive x direction.

The exact solution for ice front location x versus time t is given by Ozisik [15]. Figure 4 shows examples of numerical results calculated using FLUENT as compared to the above analytical solution. As one can see, the ice front propagation obtained by numerical solution agrees well with the analytical solution. The small difference results because the apparent heat capacity method has to assign a small “mushy” region even for a pure material.

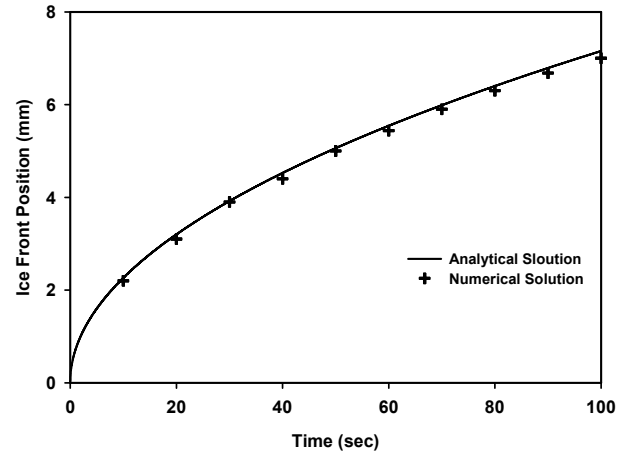


Figure 4. Comparison of analytical and numerical solutions for ice front propagation.

The grid dependence has been examined for freezing and thawing processes. The calculations on a grid with 210,000 cells are found fully convergent. All results presented in the paper are obtained with this grid.

THERMAL PROPERTIES OF SKIN TISSUES

Smith *et al.* [16] noted that the predicted thermal history of an iceball is strongly affected by temperature-dependent thermal properties. The present study estimates the thermal properties for frozen tissue by assuming that the non-water portion conducts a negligible amount of heat. Human dermis tissue consists of 65% water [14], and the temperature dependence of the thermal properties of water were taken from Alexiades and Solomon [17]. The upper limit temperature (liquidus) of the phase change region, $T_{m1} = -0.5^\circ\text{C}$, the initial freezing point of plasma [8]; and the lower limit temperature (solidus), $T_{m2} = -10^\circ\text{C}$, were obtained from Hoffman and Bischof’s work [18]. The source terms of blood perfusion and metabolic heat generation as well as the temperature dependence of the thermal properties were implemented in FLUENT by user-defined functions (UDF).

RESULTS AND DISCUSSIONS

In our model, the cooling condition of the LN_2 spray is simplified by an average heat transfer coefficient, h_s , which may vary depending on tank pressure, nozzle size, and spray distance [20]. h_s may also vary with time as the skin surface temperature decreases. Little information is available in the literature on LN_2 spray under the present configuration. Therefore, a range of values of h_s is employed in this study,

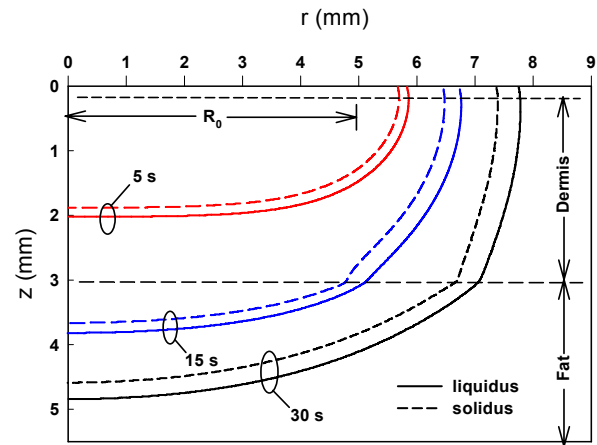
varying from 10^4 to 10^6 $W/m^2 K$, to examine the effect of h_s on iceball formation. Once spray stops, h_s is replaced by h_a , the heat transfer coefficient for air convection ranging from 10 to $50 W/m^2 K$.

During cryosurgery, iceball front propagation is the most important information for dermatologists. For any give values of h_s and h_a , the iceball front's propagation, represented by the liquidus and solidus isotherms, are therefore examined quantitatively for freezing and thawing processes with respect to time. In addition, the thermal history of tissues, the cooling rate and the lethal temperature isotherm propagation are also examined in a quantitative manner.

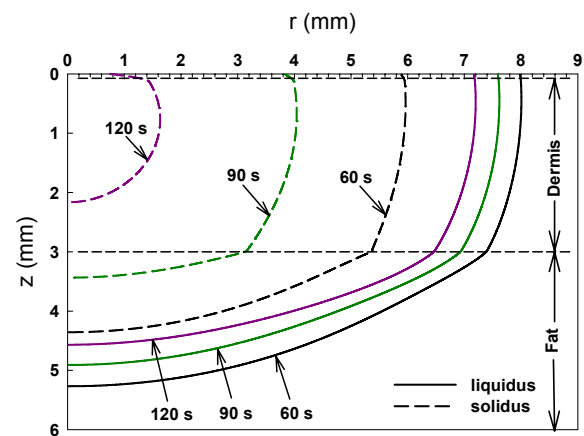
Isotherms Evolution and Penetration Depth

A typical frozen front propagation is shown in Fig. 5 by the isotherms evolution (T_{m1} and T_{m2} for unfrozen/mushy zone interface and frozen/mushy zone interface, respectively). Fig. 5a presents the propagation during the freezing process with $h_s = 10^6 W/m^2 K$ which lasts 30 seconds. It is evident that as the LN_2 spray impinges on the skin surface, isotherms start to propagate along both axial and radial directions. The propagation rate along the axial direction (i.e. the direction penetrating into the skin) occurs faster than that in the radial direction (i.e. parallel to the skin surface). Before the fronts reach subcutaneous fat (for example, $t = 5$ seconds), the isotherms are smoothly elliptic. As the spray proceeds, the fronts march through the dermis layer (for example $t = 15$ and 30 seconds) and then inflexion points appear on the isotherms at the boundary of dermis and subcutaneous fat, resulting in loss of the elliptic shape. These inflexion points arise because of the different thermal physical properties of dermis and subcutaneous fat, which changes the front propagation rate by the Stephan condition at the solid-liquid interfaces. Fig. 5b depicts isotherm evolution during the thawing process with $h_a = 10 W/m^2 K$ after the spray. It can be seen that the T_{m1} isotherm (liquidus, solid line in the figure) retreats toward the center of the spray cooling site much slower than the T_{m2} isotherm (solidus, dashed line in the figure). As a result, the narrow mushy zone formed during freezing grows considerably during the thawing process. Moreover, the geometry of solidus changes significantly from a flat quarter-ellipse to a quarter-sphere. The withdrawal of solidus occurs much faster in the epidermis than in the dermis because there is no phase change considered in the epidermis.

Careful examination of the liquidus position at 30s and 60s reveals that the liquidus does not begin retreat immediately after spray termination. Rather, the liquidus keeps propagating during the early stages of the thawing process (Fig. 6). The insert of Fig. 6 introduces penetration depth, the position of the liquidus or solidus on a central axis. Fig. 6 demonstrates that as the spray terminates at 30s, neither liquidus nor solidus have reached their maximum penetration depth, implying the propagation of iceball fronts do not stop synchronized with the spray. There is a period of approximately 10s for solidus and 20s for liquidus after termination of the spray, during which iceball front propagation continues. Ideally, cryosurgery would create an iceball encompassing the whole tumor while being



(a)



(b)

Figure 5. Iceball front propagation: (a) Freezing process with $h_s=10^6 W/m^2K$; (b) Thawing process with $h_a= 10 W/m^2K$.

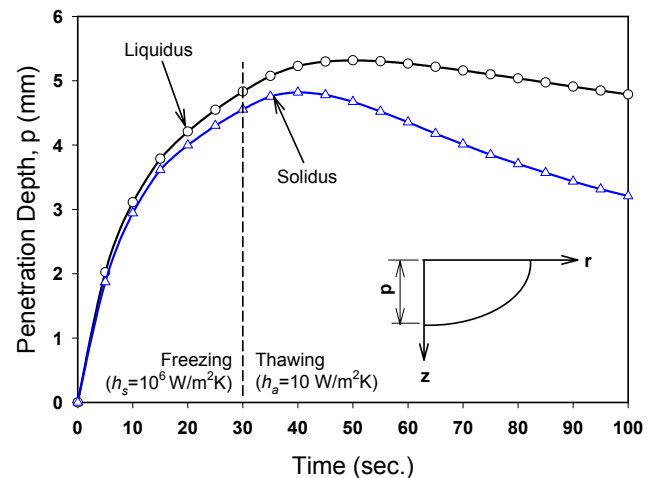


Figure 6. Penetration depths of liquidus and solidus during freezing and thawing processes.

minimally invasive to the surrounding healthy tissue. Fig. 6 reminds dermatologists that the real freezing damage will be underestimated if the cease of the frozen fronts propagation is assumed to be synchronized with that of LN₂ spray.

Besides phase change temperatures (T_{m1} and T_{m2}), another critical thermal parameter in cryosurgical quantitative analysis is the lethal temperature. Freezing tissue to or lower than the lethal temperature will completely destroy the tissue. Numerous publications have shown that lethal temperatures are highly cell and tissue type dependent, ranging from -10°C for MBT-2 bladder carcinoma [21] to -50°C in healthy skin tissue [22]. -50°C is now widely accepted as the lethal temperature for malignant skin tumors by dermatologists [23]. During cutaneous cryosurgery, one needs to know the time penetration depth of aforementioned thermal parameters in dermis tissue during freezing in order to confirm that the target tumor is entirely enclosed by lethal isotherm but healthy skin cells (like melanocytes) are not damaged. This is presented in Fig. 7, where the dimensionless penetration depth p^* and the dimensionless time τ are defined as follows:

$$p^* = \frac{p}{R_0}, \quad \tau = \frac{\bar{\alpha} \cdot t}{R_0^2} \quad (3)$$

In the definition, p is the penetration depth of the addressed isotherm along the central axis (refer to the insert in Fig. 6), R_0 is the radius of the spray cooling area, and $\bar{\alpha}$ is the temperature weighted thermal diffusivity, calculated as follows:

$$\bar{\alpha} = \frac{\bar{k}}{\rho \cdot \bar{C}} \quad (4)$$

where $\bar{\varphi} = \frac{\int_{77}^{310} \varphi(t) dt}{310-77}$ with $\varphi = k$ or C of dermis. During the

freezing process, liquidus and solidus are always close to each other in the dermis leaving a very narrow mushy zone (< 0.25 mm for $h_s=10^6$ W/m²K). Therefore, Fig. 7 only considers liquidus and lethal isotherm penetration. Regression analysis reveals that variation of p^* with respect to dimensionless time τ shows a function, which can be fitted by a cubic polynomial equation:

$$p^* = p_0 + a\tau + b\tau^2 + c\tau^3 \quad (5)$$

where the regression constants are listed in Tab. 3. As can be seen, the regression constants, p_0 , a , b and c , are functions of the convective heat transfer coefficient, h_s , when h_s is smaller than 10⁵ W/m²K. Further increasing h_s to 10⁶ W/m²K, however does not show significant change in p^* .

In clinical practice, the relative importance of phase change and lethal temperatures depends mainly on the type of target tissue. For malignant tumors, one has to make sure that all target cancerous cells are destroyed entirely by freezing, and lethal temperature isotherms should be utilized, choosing a relatively wide margin beyond the pathologic border [6]. If the target is a benign lesion, it is of primary importance to limit freeze injury of healthy tissue, for example protect melanocytes from permanent injury to avoid hypopigmentation. In this case, a much smaller margin or even no margin is desired, and phase change temperature isotherms can be used to achieve this goal.

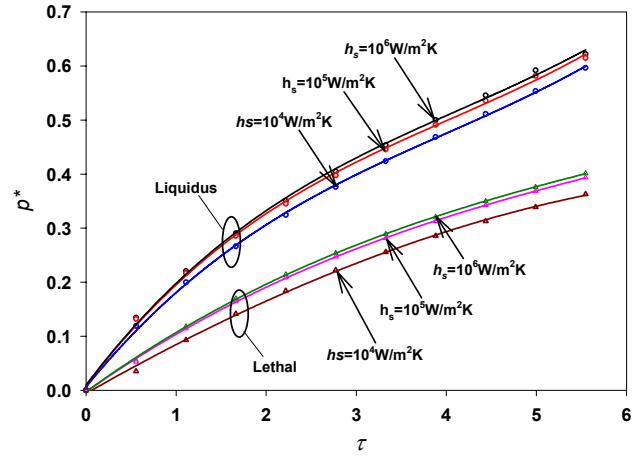


Figure 7. Penetration depth of liquidus and lethal isotherms in dermis during freezing.

Table 3. Regression constants for penetration depth of liquidus and lethal isotherms.

Isotherm	h_s (W/m ² K)	p_0	a	b	c
Liquidus	10 ⁴	0.0063	0.20	-0.036	0.0027
	10 ⁵	0.0089	0.22	-0.036	0.0030
	10 ⁶	0.0096	0.22	-0.035	0.0028
Lethal	10 ⁴	-0.0060	-0.095	-0.0047	-0.00010
	10 ⁵	-0.0030	0.12	-0.011	0.00055
	10 ⁶	-0.0028	0.12	-0.012	0.00055

Equation 5 with Tab. 3 can therefore be used by cryosurgeons for quantitative evaluation of freezing effect in early planning.

Thermal History during Freezing and Thawing

Besides the achievement of lethal temperature, thermal history of a cell, including cooling rate and hold time (the duration a cell is maintained at or lower than the lethal temperature), plays an equally important role for cellular injury [21].

It is well accepted now that two biophysical events may cause cell injury and death during freezing: cell dehydration by water transport across the cell membrane (i.e. solute or solution effects), and IIF. When cells together with their extracellular matrix are cooled below the phase change temperature, ice forms extracellularly, and the solute concentration outside the cell begins to increase. If the cooling rate is low, intracellular water has sufficient time to diffuse through the plasma membrane to balance the osmotic pressure difference between intracellular and extracellular spaces. As a result, cells become dehydrated and intracellular solutes are highly concentrated. This results in damage to cellular proteins and enzymatic systems, and destabilization of cell plasma membranes. On the other hand, if the cooling rate is high, intracellular water has little time to leave the cell, ice nucleates inside the cell and IIF occurs. IIF causes injury to cell membranes and is thought to damage cellular organelles and cytoskeletons [24].

Figure 8 presents the typical tissue temperature variation during the freeze-thaw process at several different locations along the central axis as measured from the skin surface: $z = 0$,

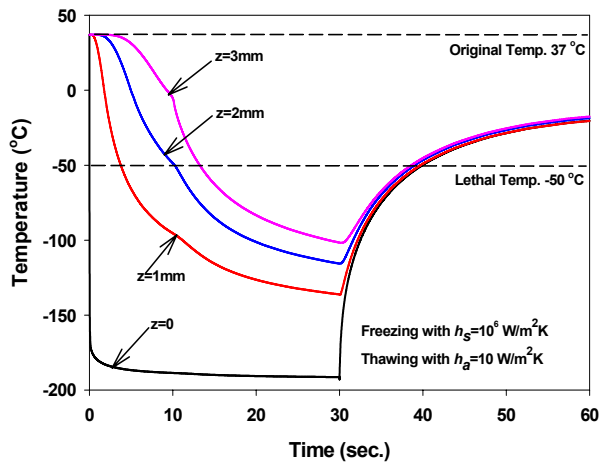


Figure 8. Temperature variation for skin surface and dermis tissue during freezing-thawing process.

1, 2, and 3 mm. The convective heat transfer coefficient is fixed at $10^6 \text{ W/m}^2 \text{ K}$, a fairly high value for freezing and $10 \text{ W/m}^2 \text{ K}$ for thawing. It is evident that it takes less time for the skin surface to reach the lethal temperature as compared to deeper regions. Therefore, while tissue close to the skin surface cools rapidly leading to IIF, deeper layers experience much slower cooling rates, allowing equilibration of solutes between the intra and extracellular compartments and resultant cellular dehydration. Furthermore, in the superficial dermis, as intracellular ice remains below the phase change temperature for a longer period (124s for the cell at $z = 1\text{mm}$), recrystallization of ice (fusion to form larger crystals which decreases the surface area and minimizes free energy) may occur. This would result in disruption of cell membranes or organelles [21]. Three cooling curves ($z = 1, 2$ and 3 mm) show inflexion points at approximately 10s, when ice fronts reach the boundary between dermis and fat. Once ice fronts move into fatty tissue, phase changes occur. Water content of the dermis is 65%, a significant difference compared to subcutaneous fat where water content is only 21% [15]. This results in much lower latent heat in the fat as compared to the dermis. A sudden drop occurs in the total latent heat liberation rate when ice fronts move into the subcutaneous fat layer, further changing the cooling rates of the frozen dermis tissue. Investigation of thermal history using $h_s = 10^4 \text{ W/m}^2 \text{ K}$ reveals that the inflexion points on cooling curves also occur when ice fronts reach the dermal/fat boundary. It is also evident from Fig. 8 that, temperature distribution is more uniform in the thawing dermis as compared to the frozen section. Recall that the epidermis and subcutaneous fat have much lower thermal conductivity than the dermis.

Figure 9 shows temperature variations during the first seconds of the thawing process. Two air convective heat transfer coefficients are considered: the solid line represents the solution using $10 \text{ W/m}^2 \text{ K}$ and the dotted line represents results using $50 \text{ W/m}^2 \text{ K}$. As one can see, use of the higher convective heat transfer coefficient results in more rapid warming of the skin surface ($z=0$), but has less of an effect on deeper dermal tissue ($z = 1, 2$ and 3 mm). Evaluation of the thawing process at

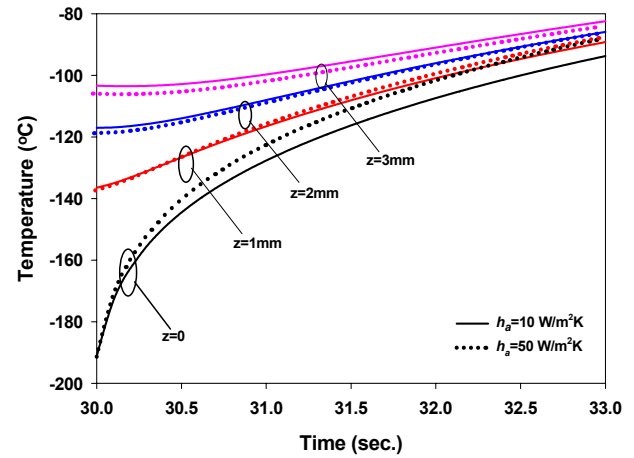


Figure 9. Effect of air convection heat transfer coefficients on tissue temperature variation during the beginning of thawing process.

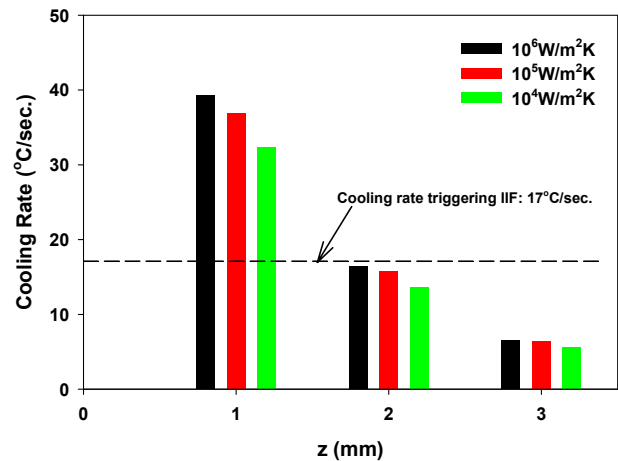


Figure 10. Cooling rates underneath skin surface when temperature drops to liquidus temperature, T_{m1} .

300s reveals that the temperature differences caused by these two heat transfer coefficients are only $6.1 \text{ }^\circ\text{C}$, $5.4 \text{ }^\circ\text{C}$, and $5.3 \text{ }^\circ\text{C}$ for dermal tissue at $z = 1, 2$ and 3 mm , respectively.

As Fig. 8 demonstrates, tissue cooling rate is highly location dependent. It is therefore necessary to discuss cooling rate as a function of space, as shown in Fig. 10, where each bar represents the cooling rate when the temperature drops to liquidus temperature, T_{m1} , the moment phase change (ice formation) starts. For convenience, it is assumed that IIF occurs once the cooling rate exceeds $1000 \text{ }^\circ\text{C/min}$ ($\approx 17 \text{ }^\circ\text{C/s}$), a calculated result from Mazur *et al* [25]. It can be seen that when tissue temperature drops to T_{m1} , the cooling rates at 1 mm beneath the skin surface exceed $17 \text{ }^\circ\text{C/s}$, while those at 2 mm and 3 mm do not. One can therefore expect that the IIF region will occur in cells 1 mm beneath the skin surface or less while cells located at 2 mm and deeper are more likely to witness extracellular ice formation and, therefore, suffer cellular dehydration.

CONCLUSIONS

A mathematical model has been developed for LN₂ cutaneous cryosurgery. Considering the multilevel structure of human skin, the computation domain consists of three distinct layers: epidermis, dermis and subcutaneous fat. Freezing and thawing of dermis and fatty tissues are assumed to take place over a temperature range from -0.5 °C to -10 °C. Blood perfusion and metabolism are considered in unfrozen dermis. During the freezing process, the heat transfer between the epidermis and sprayed LN₂ is simplified by a convective heat transfer coefficient, h_s , with the LN₂ film on the skin surface assumed to be at saturation temperature and atmospheric pressure. For thawing, the model uses air convective heat transfer coefficient, h_a , with room temperature. The model allows detailed evaluation of iceball formation during cutaneous cryosurgery and propagation of lethal temperature isotherms. During freezing, iceball front isotherms are found spatially inhomogeneous, progressing rapidly axially and more slowly laterally. Examination of the thermal history shows that targeted tissues at different depths have different cooling rates, and therefore will experience varied injury mechanisms. For example, along the central axis, rapid LN₂ cooling will induce IIF for cells approximately 1mm from the skin surface or less, while slower cooling of cells 2 mm or more from the surface may result in cellular dehydration. Post-LN₂ application, iceball front propagation does not stop immediately. During the thawing process, the solidus isotherm withdraws much faster than liquidus, resulting in significant enlargement of the mushy zone. Use of a higher convective heat transfer coefficient, h_a , speeds up warming at the skin surface, but functions less for deeper dermal tissue. Such information can be used for pretreatment planning and optimization of LN₂ spray cryosurgical protocols of skin and eventually, other organs.

REFERENCES

1. Kuflik, E. G., 1994, "Cryosurgery updated," *Journal of the American Academy of Dermatology*, Volume 31, No. 6, pp. 925-944
2. Korpan, N. N., 2001, *Basics of Cryosurgery*, Springer-Verlag / Wien York.
3. Cooper, T. E. and Trezek, G. J., 1972, "On the Freezing of Tissue," *Journal of Heat Transfer*, Vol. 94, pp. 251-253.
4. Zacarian, S. A., 1973, *Cryosurgery of Tumors of the Skin and Oral Cavity*, Charles C Thomas, pp.
5. Graham, G. F., 2001, "Cryosurgery in the Management of Cutaneous Malignancies," *Clinics in Dermatology*, Vol. 19, pp. 321-327
6. Andrews, A. D., 2004, "Cryosurgery for Common Skin Conditions," *American Family Physician*, Vol. 69, No. 10, pp. 2365-2372
7. Pennes, H. H., 1948, "Analysis of Tissue and Arterial Blood Temperatures in the Testing Human Forearm," *Journal of Applied Physiology*, Vol. 1, No. 2, pp. 93-122
8. Comini, G. and Giudice, S. D., 1976, "Thermal Aspects of Cryosurgery," *Journal of Heat Transfer*, Vol. 98, pp. 543-549.
9. Rubinsky, B. and Shitzer, A. 1976, "Analysis of a Stefan-like problem in a Biological Tissue around a Cryosurgical Probe," *Journal of Heat Transfer*, Vol. 98, pp. 514-519.
10. Rubinsky, B., 2000, "Cryosurgery," *Annual Review of Biomedical Engineering*, Vol. 2, pp. 157-187.
11. Cooper, I. S., 1967, *Engineering in the Practice of Medicine*, Williams & Wilkins, Baltimore, pp. 122-140
12. W. Franco, J. Liu, G-X. Wang, J.S. Nelson and G. Aguilar, 2005, "Radial and Temporal Variations in Surface Heat Transfer during Cryogen Spray Cooling," *Physics in Medicine and Biology*, Vol. 50, pp. 387-397.
13. Hoffmann, N. E. and Bischof, J. C., 2001, "Cryosurgery of Normal and Tumor Tissue in the Dorsal Skin Flap Chamber: Part I - Thermal Responses," *Journal of Biomedical Engineering*, Vol.123, pp. 301-309
14. Duck, F. A., 1990, *Physical Properties of Tissue*, Academic Press, San Diego.
15. Ozisik, M. N., 1993, *Heat Conduction* (2nd Edition), John Wiley & Sons, New York.
16. Smith, D. J., Devireddy, R. V. and Bischof, J. C., 1999, "Prediction of thermal history and interface propagation during freezing in biological systems -Latent heat and temperature-Dependent property Effects," Proc. 54th ASME/JSME Joint Thermal Engineering Conference, San Diego, CA.
17. Alexiades, A. and Solomon, A. D., 1993, *Mathematical Modeling of Melting and Freezing Processes*, Hemisphere, Washington D.C.
18. Hoffmann, N. E. and Bischof, J. C., 2001, "Cryosurgery of Normal and Tumor Tissue in the Dorsal Skin Flap Chamber: Part I - Thermal Responses," *Journal of Biomedical Engineering*, Vol.123, pp. 301-309.
19. Shitzer, A. and Eberhart, R. C., 1985, *Heat Transfer in Medicine and Biology (I)*, Plenum Press, New York.
20. Aguilar, G., Wang, G-X. and Nelson, J. S., 2003, "Effect of Spurt Duration on the Heat Transfer Dynamics during Cryogen Spray Cooling," *Physics in Medicine and Biology*, Vol. 48, pp. 2169-2181.
21. Hoffmann, N. E. and Bischof, J. C., 2002, "The Cryobiology of Cryosurgical Injury," *Urology* (Supplement 2A), Vol. 60, pp. 40-49.
22. Gage, A. A., Caruana, J.A. and Montes, M., 1982, "Critical Temperature for Skin Necrosis in Experiment Cryosurgery," *Cryobiology*, Vol. 19, pp. 273-282.
23. Committee on Guidelines of Care, 1994, "Guidelines of care for cryosurgery," *Journal of the American Academy of Dermatology*, Vol. 31, pp. 648-653.
24. He, X. and Bischof, J. C., 2003, "Quantification of Temperature and Injury Response in Thermal Therapy and Cryosurgery," *Critical Review in Biomedical Engineering*, Vol. 31, pp. 355-421.
25. Mazur, P. and Koshimoto, C., 2002. "Is Intracellular Ice Formation the Cause of Death of Mouse Sperm Frozen at High Cooling Rate?" *Biology of Reproduction*, Vol. 66, pp. 1485-1490.